Hindawi
Geofluids
Volume 2023, Article ID 3747027, 9 pages
https://doi.org/10.1155/2023/3747027

Research Article

Creep Behavior and Its Prediction of Saturated Weakly Cemented Medium-Grained Sandstone under Multiaxial Loadings

Qingheng Gu,[1,2] Guangming Zhao,[1,2] Xiangrui Meng,[1,2] Jian Sun,[1,2] Xiang Cheng,[1,3,4] Wensong Xu,[1] and Ruofei Zhang[1,2]

[1]*State Key Laboratory of Mining Response and Disaster Prevention and Control in Deep Coal Mines, Anhui University of Science and Technology, Huainan 232001, China*
[2]*School of Mining Engineering, Anhui University of Science and Technology, Huainan 232001, China*
[3]*Mining Engineering Post-Doctoral Flow Station, Anhui University of Science and Technology, Huainan 232001, China*
[4]*Post-Doctoral Research Station, Huainan Mining Industry (Group) Co., Ltd., Huainan 232001, China*

Correspondence should be addressed to Guangming Zhao; 1090047040@qq.com

Received 7 October 2022; Revised 7 November 2022; Accepted 26 November 2022; Published 6 February 2023

Academic Editor: Zhengzheng Xie

Weakly cemented medium-grained sandstone in Ordos mining area of China is widely distributed under phreatic water. The creep behavior of saturated rock is important for the stability of water-resisting strata. In this paper, creep mechanical properties of saturated medium-grained sandstone were studied by triaxial rheological test. The results showed that medium-grained sandstone only shows attenuation creep and stable creep under low stress level, and accelerated creep occurs when axial load reaches about 75% of instantaneous compressive strength. The rock samples exhibit volume dilatancy under most loading levels and finally shear fracture. The failure mechanism is the dislocation separation of mineral particles. Based on the energy dissipation theory, the damage evolution equation was modified and introduced into the Burgers model, which can accurately describe the rheological behavior of saturated medium-grained sandstone. The modified model was used to predict the crack initiation time under different deviatoric stresses, which can provide guidance for early warning of water-resisting rock stability.

1. Introduction

A special rock material, medium-grained sandstone, widely exists under phreatic water in Ordos mining area of Western China. This rock material is of late diagenesis, which results in the poor cementation of rock particles and low strength of rock [1–3]. The climate in this area is dry, and there is precious phreatic water above the weakly cemented rock stratum [4, 5]. Therefore, when mining coal seams under weakly cemented water-resisting strata, not only the long-term stability of medium-grained sandstone affected by groundwater should be paid attention to, but also the early warning method of rock fracture instability needs to be studied.

Groundwater has a great influence on mechanical properties of soft rocks [6–17]. For example, Yao et al. [6] carried out uniaxial compression and acoustic emission monitoring tests of coal with different water contents. The results showed that the strength and deformation modulus of coal after water immersion decrease with the increase of water content, and the fracture evolution of coal can be predicted by acoustic emission signal. Fabre and Pellet [7] studied the creep characteristics of three types of sedimentary rocks by using uniaxial compression creep test and pointed out that isokinetic creep and accelerated creep would occur only when the stress exceeded a certain value; otherwise, the rock would only show deceleration creep. Cao et al. [8] studied

the creep characteristics of anorthosite under water-saturated and air-dried conditions through uniaxial compression creep tests and pointed out that it takes longer for saturated rocks to achieve stable creep than air-dried rocks. Yan et al. [9] analyzed the creep experimental results of granite under different stresses and osmotic pressures and modified the Nishihara model. The results showed that the improved Nishihara model could better describe the whole process and nonlinear characteristics of rock creep. In a word, water will weaken the mechanical properties of rocks. With the increase of water content, the strength and deformation resistance of rock gradually decrease, and the creep rate increases under long-term load, and the duration of stable creep extends. Therefore, it is impossible to find a unified law of the influence of water on rock creep behavior with different water-weakening properties. The creep properties of weakly cemented medium-grained sandstone under the influence of water need to be studied specifically.

In addition, the stability evaluation of water-resisting strata is important to ensure the safety of mining. The signs of rock failure can be obtained by abnormal deformation or external monitoring [18–22], but they are not suitable for failure prediction considering rock anisotropy. The creep model can be used to describe the relationship between rock deformation and time, and rock deformation is related to the development of cracks [23]. So the failure behavior of rock can be predicted by using creep model. Up to now, most creep models have been studied to accurately describe the existing test or field behavior [24–28]. However, the accuracy of using creep model to make further prediction remains to be demonstrated, especially to link fracture prediction with creep deformation.

In this paper, the weakly cemented water-resisting medium-grained sandstone was taken as the research object. The water-resisting rock mass in daily water environment can be considered as saturated. The creep mechanical properties of saturated rock samples under different confining pressures were experimentally studied to obtain its unique rheological properties. The damage evolution equation and creep model based on energy dissipation were improved, and a prediction method of rock cracking initiation point in creep process was proposed.

2. Experimental Method

2.1. Sample Preparation. The mineral components of the rock mainly include quartz, illite, chlorite, and albite, with the contents of 27.75%, 16.18%, 8.09%, and 47.98%, respectively. Illite and chlorite belong to clay minerals. That is to say, the clay mineral content of the medium-grained sandstone studied is about 24%.

Medium-grained sandstone is mainly composed of mineral particles (MP), which are connected by clay minerals (Figure 1). Most mineral particles are irregular aggregates, and some unconformity contact between particles forms original defects in the sample, which contributes to the time-dependent behavior of rocks and crack initiation [29].

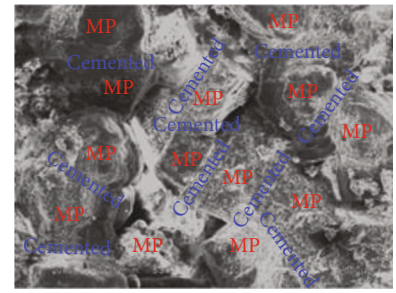

Figure 1: Photomicrographs of the internal structure of medium-grained sandstone.

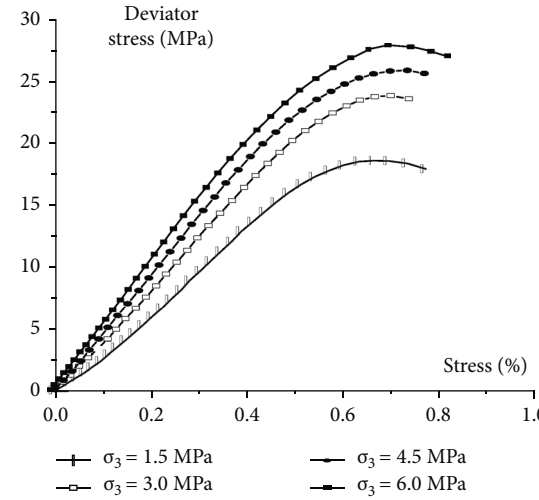

Figure 2: Stress-strain curves of saturated medium-grained sandstone under triaxial compression.

The saturated samples of medium-grained sandstone for the test were prepared according to the procedure outlined by ISRM [30]. The ratio of height to diameter of specimens is 2 : 1, and the diameter is about 50 mm. The height is about 100 mm, and the error of the surface roughness is less than 0.02 mm. The production process of saturated rock samples is to immerse the dry rock in clean water, weigh it every half an hour within the first 10 hours, and then weigh it every hour until its mass remains unchanged [12].

2.2. Axial Load Classification. The creep test adopts the graded loading method, and the compressive strength of the rock under the corresponding confining pressure needs to be tested before the classification of the graded loading creep level. The confining pressure (σ_3) was designed as 1.5 MPa, 3.0 MPa, 4.5 MPa, and 6.0 MPa. The triaxial compression stress-strain relationship of rock under four confining pressures is shown in Figure 2. The compressive strength of saturated sample is 18.6 MPa, 23.8 MPa, 26.8 MPa, and 29.3 MPa with σ_3 of 1.5 MPa, 3.0 MPa, 4.5 MPa, and 6.0 MPa.

The axial load of the test starts from about 50%-60% of the compressive strength. The difference between two adjacent loads is 2.0 MPa. The specific implementation scheme is shown in Table 1.

Table 1: Implementation scheme of creep test for medium-grained sandstone.

Rock sample	σ_3 (MPa)	σ_1-σ_3 (MPa)							
Saturated medium-grained sandstone	1.5	9.5	11.5	13.5	15.5	17.5	19.5	21.5	…
	3.0	12	14	16	18	20	22	24	…
	4.5	14.5	16.5	18.5	20.5	22.5	24.5	26.5	…
	6.0	15	17	19	21	23	25	27	…

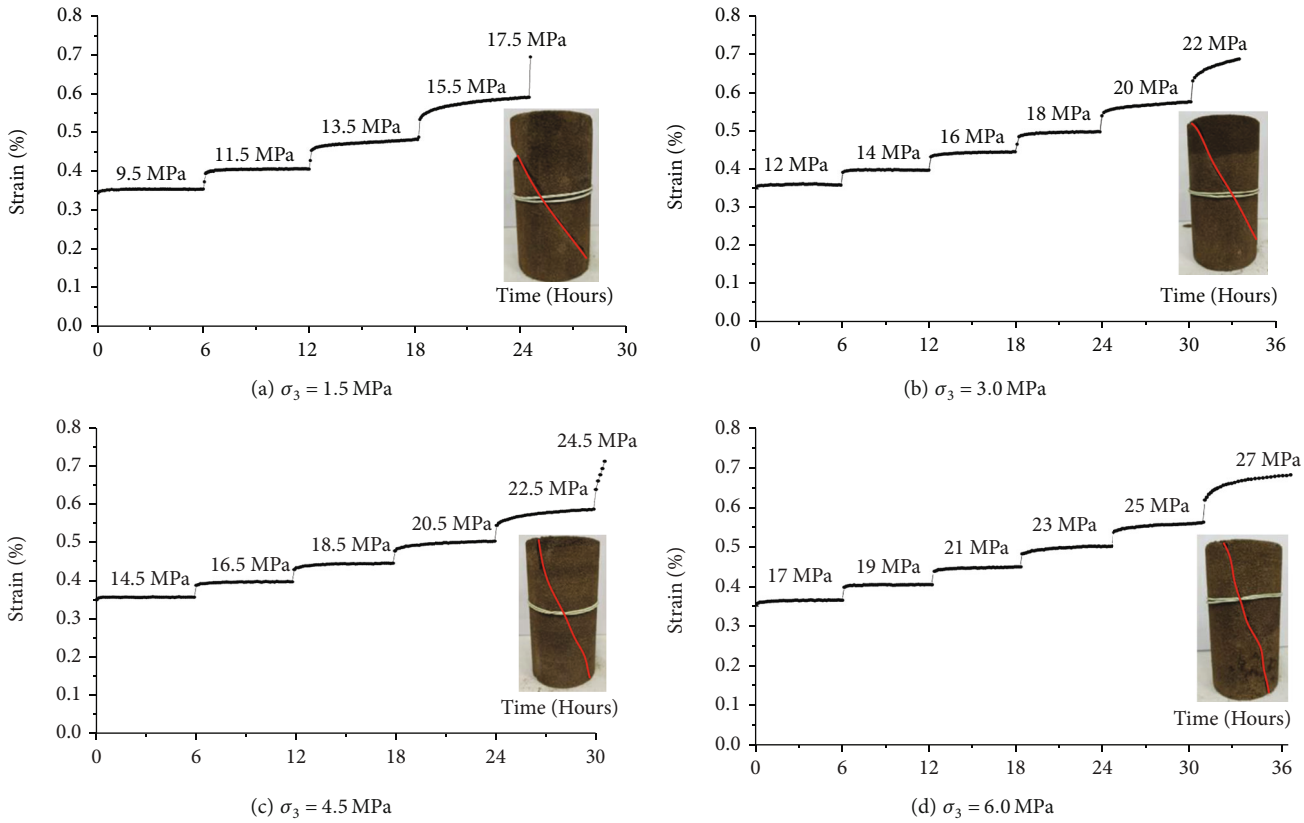

Figure 3: Strain curves in a multiloading triaxial creep test.

2.3. Creep Test Equipment and Procedures. Triaxial creep test was carried out on RLJW-2000 servo-controlled testing machine [31, 32]. At the beginning of the test, the confining pressure is loaded to the set value at the rate of 0.05 MPa/s, and then, the axial deviating stress is loaded to the first level at the rate of 0.06 mm/min. The axial pressure is maintained for 6 hours before loading to the next level and so on until the specimen is destroyed.

3. Results and Discussion

3.1. Time-Dependent Strain of Medium-Grained Sandstone. The variation of axial creep deformation of saturated medium-grained sandstone with time is shown in Figure 3. The specimen produces obvious instantaneous deformation when each level of deviator stress is applied. The instantaneous strain of the specimen is the largest when the first loading level is applied, and the subsequent instantaneous deformation increases with the increase of the loading level. When the confining pressure is different, the application of the first-order load has little effect on the instantaneous strain, which is about 0.35%, indicating that the compression effect of about 60% compressive strength on saturated medium-grained sandstone is basically the same.

When the deviator stress is less than 75% of the compressive strength, the rock sample only shows instantaneous deformation and decay creep, and the rock deformation reaches a stable state in a short time. When the deviator stress increases to a certain extent, the rock deformation shows obvious time correlation, and it takes a long time for the rock deformation to reach a stable state. With the increase of loading level, the steady-state creep rate of rock (slope of line segment in steady-state deformation stage) gradually increases until accelerated creep occurs. Macroscopic fracture instability occurs in a short time after the start of accelerated creep.

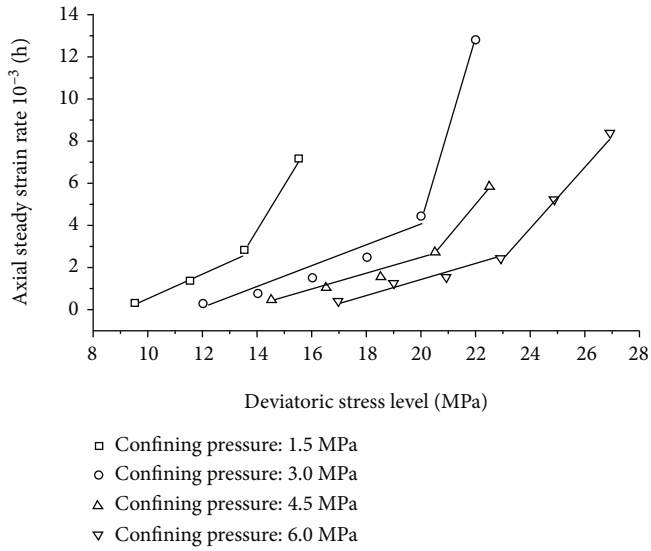

Figure 4: Relationship between steady strain rate and deviatoric stress.

3.2. Strain Rate Analysis. The creep rate of rock can indirectly reflect its damage and fracture state. If the internal cracking of rock is serious, the creep rate of rock will increase obviously. The creep rate of rock samples under different deviatoric stresses and confining pressures is shown in Figure 4. Under the same confining pressure, the stable creep rate of rock increases with the increase of deviatoric stress. Before the last stage of loading, the creep rate increases linearly with the deviatoric stress. At the last stage of loading, the creep rate increases rapidly, which indicates that the cracks in the rock expand, and the bearing capacity of the rock weakens.

It can also be seen from Figure 4 that the stable creep rate of rock with large lateral restraint is also large, but the difference of creep rate between two adjacent loading levels is slightly smaller. This reminds us that in practical engineering, support and reinforcement can effectively improve confining pressure and long-term stability of the project.

3.3. Fracture Characteristics. The damage and fracture of rock are interrelated. In fact, the damage process of rock is a process in which cracks gradually initiate, expand, and coalesce to form macrofractures. The damage in this process grows slowly first and then rapidly to 1 [31]. The fracture morphology of saturated medium-grained sandstone is shown in Figure 3. Shear failure occurs in the rocks under four confining pressures. The rock with high confining pressure has a small fracture angle; that is, when the lateral restraint is small, the rock shear angle is large, resulting in large shear deformation.

To further understand the fracture mechanism of medium-grained sandstone, the fracture appearance of rock is scanned, and the scanning image is shown in Figure 5. Compared with Figure 1, it can be seen that the fracture of rock is mainly caused by the dislocation of mineral particles, which eventually leads to the formation of macrofracture surface. This is mainly due to the small cementation between

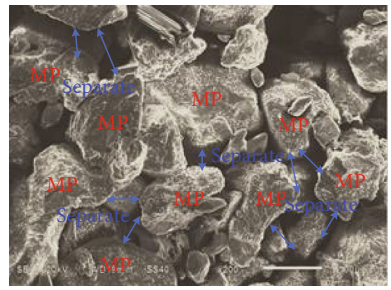

Figure 5: Photomicrographs of the fracture appearance of medium-grained sandstone.

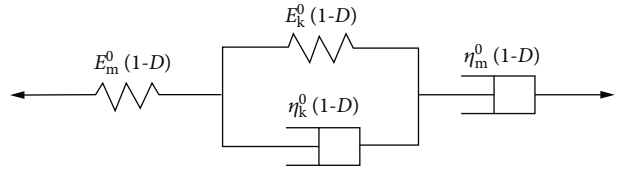

Figure 6: Burgers model considering damage.

mineral particles, which is easy to fail under high pressure and long time. This is also the difference between weakly cemented rock and some macroscopic rock damage caused by mineral particle fracture.

3.4. Creep Behavior Prediction

3.4.1. Creep Model Analysis. The constitutive model can describe the deformation and failure process of rock. For medium-grained sandstone, the rock presents deceleration creep and steady creep under deviating stress, i.e., linear creep. This creep behavior can be well described by the Burgers model [26]. However, the development of rock failure mainly occurs in the accelerated creep stage, so a Burgers model considering damage can be used to describe the fracture process, as shown in Figure 6.

Table 2: Creep model parameters of saturated medium-grained sandstone.

σ_1-σ_3 (MPa)	σ_3 (MPa)	υ	σ_{cr} (MPa)	E_m^0 (GPa)	η_m^0 (GPa*h)	$E0$ k (GPa)	η_k^0 (GPa*h)	α	β	U_0^d (MJ/m^3)
22.0	3.0	0.40	10.5	4.02	2.42	122.14	265.49	6.35^*10^{-26}	7.28	508.71
27.0	6.0	0.34	18.3	5.21	3.01	151.45	636.10	9.26^*10^{-47}	8.14	120.54

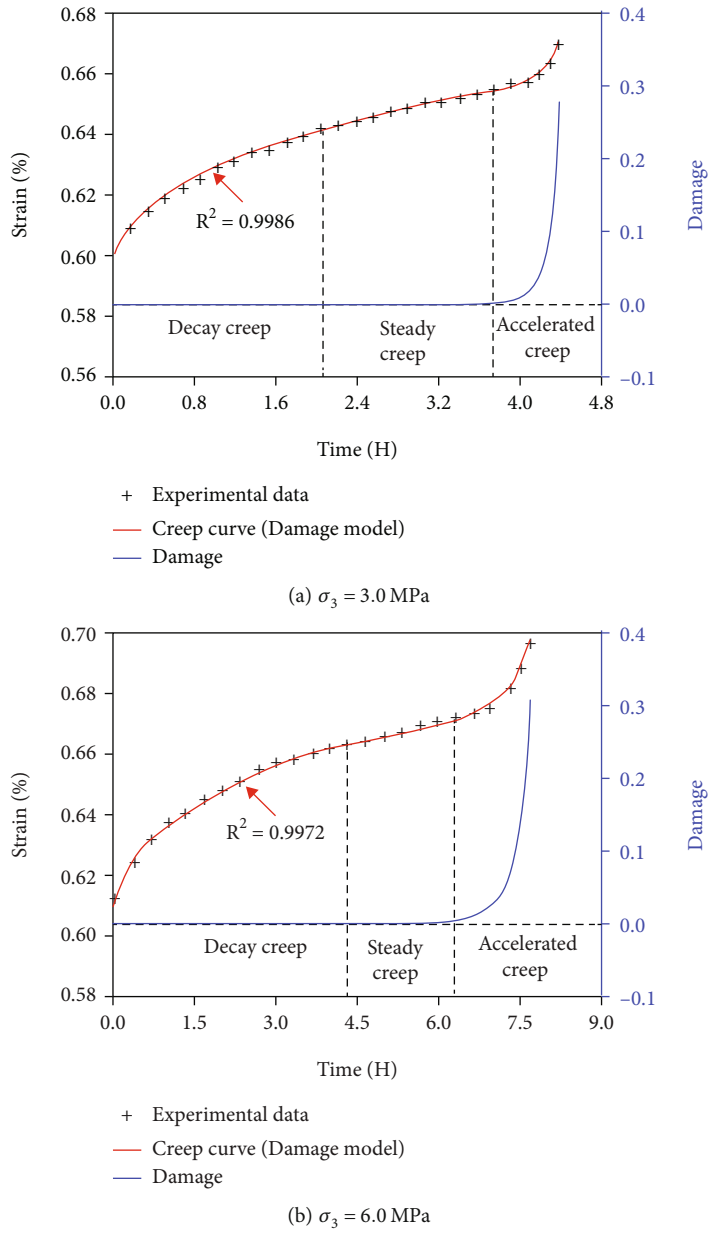

Figure 7: Comparison between damage creep model curve with the experimental result of saturated medium-grained sandstone.

As we all know, rock fracture propagation is a process of energy accumulation and dissipation [33–38]. When the energy accumulated at the crack tip reaches the energy required for its expansion, the rock fracture will expand. Xie [39] regards the microcracks and microvoids in rock as initial damage and puts forward the rock damage evolution equation based on energy expression.

$$D = 1 - \exp\left[-\alpha\left(U^d - U_0^d\right)^{\beta}\right], \quad (1)$$

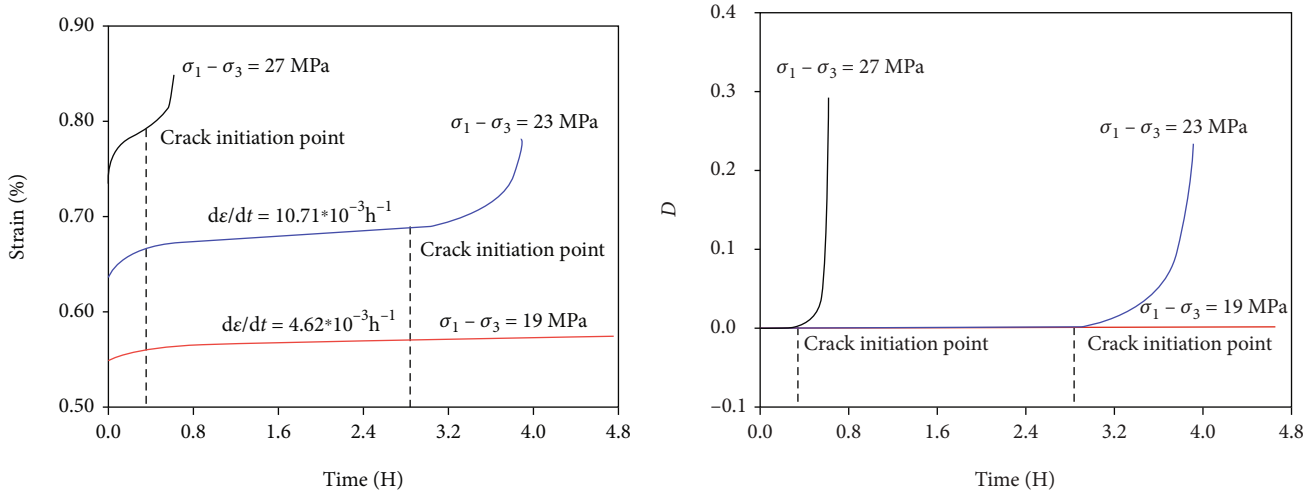

(a) Creep curve (b) Damage evolution curve

Figure 8: Damage creep model curves of saturated medium-grained sandstone under different deviatoric stress conditions (σ_3 = 3.0 MPa).

where α and β are the parameters related to the material properties, U_0^d is the energy dissipation value corresponding to the initial defect, and U^d is the energy dissipation in the process of crack propagation.

In the initial stage of loading, the dissipated energy U^d of rock is less than U_0^d, which makes the base part of exponential function $(U^d - U_0^d)$ in equation (1) less than zero. That is, the exponential function is not tenable. Therefore, the ratio of U^d to U_0^d is compared with 1 to judge whether the exponential function is tenable or not. And then, the square of $U^d/U_0^d - 1$ is taken as the base number of the exponential function, which not only eliminates the meaningless situation of the exponential function but also makes the formula de unit. Thus, the damage evolution equation based on formula (1) is obtained.

$$D = 1 - \exp\left\{-\alpha\left[\left(\frac{U^d}{U_0^d} - 1\right)^2\right]^\beta\right\}. \tag{2}$$

Under constant axial load, the dissipation energy U^d of rock can be expressed as follows [32]:

$$U^d = \frac{2(1+\nu)}{3}(\sigma_1 - \sigma_3)\varepsilon, \tag{3}$$

where σ_1 and σ_3 are axial pressure and confining pressure, υ is the Poisson's ratio of rock, and ε is the strain.

Therefore, the constitutive equation of the Burgers model considering damage can be expressed as follows [40]:

$$\varepsilon = \frac{\sigma - D\sigma_{cr}}{1-D}\left[\frac{1}{E_m^0} + \frac{1}{\eta_m^0} + \frac{1}{E_k^0}\left(1 - e^{-E_k^0/\eta_k^0 t}\right)\right], \tag{4}$$

where t is time; E_m^0, η_m^0, E_k^0, and η_k^0 are viscoelasticity coefficients of the Burgers model; and σ_{cr} is the residual strength.

The initial damage of rock is closely related to the compaction stage of prepeak stress-strain curve. Because the creep behavior of rock in this study was constrained by confining pressure, the primary void of rock decreases under confining pressure, and the prepeak compaction stage of rock was not obvious. That is, the initial damage decreases. Under uniaxial or very small confining pressure, the initial damage of rock is obvious. The application effect of the modified model in this paper will be better.

3.4.2. Creep Behavior Prediction. It can be seen from Figure 3 that the saturated medium-grained sandstone with confining pressure of 3.0 MPa and 6.0 MPa has obvious accelerated creep phenomenon. We use the modified creep model to fit the test data; the related parameters and fitting parameters of the Burgers model with damage are shown in Table 2. The fitting results are shown in Figure 7. The model was found to be suitable to describe the experimental data with good accuracy ($R^2 > 0.99$). This shows that the modified model can accurately describe the creep behavior of medium-grained sandstone, especially the accelerated creep behavior.

To explore the evolution law of rock fracture in the process of rheology, the parameters of U_0^d, α, and β are introduced into formula (2), and the damage evolution curve under the failure load level can be obtained, as shown in Figure 7. It shows that the damage variable D almost remains unchanged at the stage of deceleration creep and stable creep, which is approximately equal to 0. The damage variable D increases exponentially with the strain in the accelerated creep stage. This indicates that the rock crack almost does not expand in the decay and stable creep stages but expands exponentially in the accelerated creep stage.

To study the damage evolution of rock under different loading levels, the creep characteristics of medium-grained sandstone under different deviator stresses are predicted

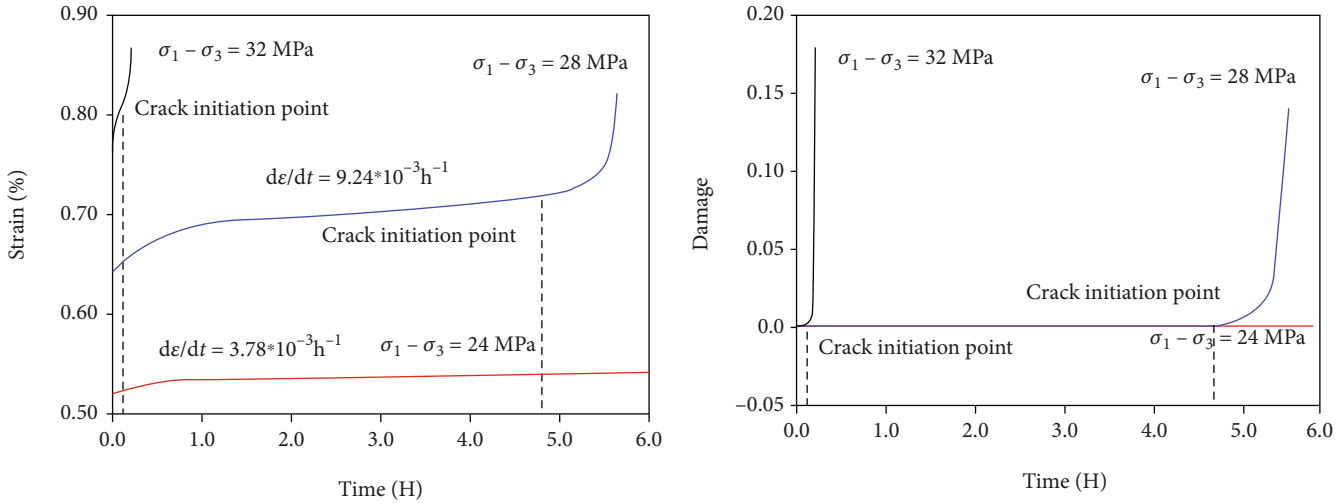

(a) Creep curve

(b) Damage evolution curve

Figure 9: Damage creep model curves of saturated medium-grained sandstone under different deviatoric stress conditions (σ_3 = 6.0 MPa).

based on the creep constitutive equation (formula (2)-formula (4)). The creep and damage evolution curves are shown in Figures 8 and 9. When the axial loading is not large enough, the creep rate of rock is low, and the damage variable is close to 0. The microcracks will not expand. The accelerated creep phenomenon of rock gradually appears with the increase of deviator stress. The greater the deviator stress is, the greater the steady creep rate is and the earlier the exponential accelerated creep occurs. The point at which the rock enters into the accelerated creep or the point at which the damage begins to increase can be regarded as the point of crack initiation. For example, when the confining pressure is 3.0 MPa and the deviator stress is 23 MPa, the accelerated creep behavior, i.e., the rock begins to fracture, occurs at t = 2.85 h, and the crack initiation point occurs at t = 0.36 h when the deviatoric stress is 27 MPa. The creep curve of rock under constant load of 23 MPa is close to that of test under 22 MPa, and the time of steady creep rate increasing slightly and entering accelerated creep is slightly earlier. This is consistent with the objective law, which shows that this method is reliable for predicting the initiation or acceleration creep time of rock materials. We can give early warning of rock and engineering based on this moment.

Because we cannot get the internal structure of rock in real time during the experiment, we can only show the failure process of rock visually by virtue of the damage evolution law of rock. Therefore, we simplified the creep fracture process of water-saturated sandstone, as shown in Figure 10. Under the low axial loading, the rock only shows the phenomena of attenuation creep and stable creep. The micropores and microcracks of rock are gradually compressed, and no new fracture occurs. When the axial load reaches about 80% of the instantaneous compressive strength, the rock begins to appear accelerated creep. The rock fracture develops exponentially, and finally, macroshear failure occurs.

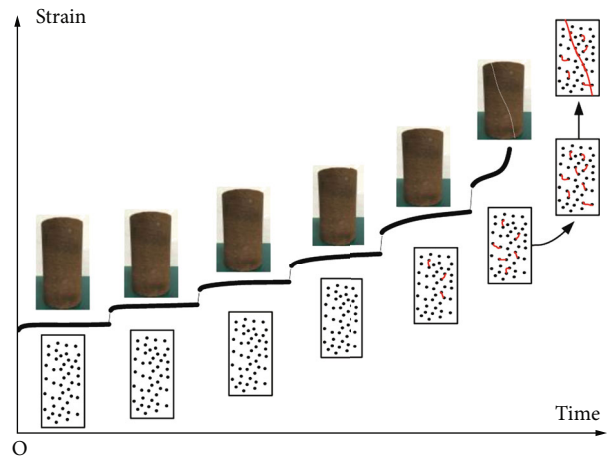

Figure 10: Fracture development process of saturated medium-grained sandstone under multiaxial loadings.

4. Conclusions

The main purpose of this study is to investigate the triaxial creep behavior of saturated medium-grained sandstone, which represents the extreme state of water-resisting rock mass. The damage variable and creep model were improved to describe the creep behavior of rock and determine the initiation time of rock fracture.

(1) The first-loading instantaneous deformation of saturated rock samples under different confining pressures is similar, and then, the instantaneous deformation increases with the increase of deviator stress. Under low stress level, medium-grained sandstone only shows attenuation creep and stable creep, and accelerated creep occurs when axial load reaches about 75% of instantaneous compressive strength

(2) Shear failure of rock samples occurs under different confining pressures, and the failure mechanism is dislocation separation between mineral particles

(3) The creep rate increases rapidly at the loading level of fracture. Based on the energy dissipation, the damage evolution equation was modified and introduced into the Burgers model, which can accurately describe the rheological behavior of saturated medium-grained sandstone. The modified model was used to predict the crack initiation time under different deviatoric stresses, which can provide guidance for early warning of rock stability

(4) The creep damage model modified in this paper is theoretically suitable for describing other rocks, especially the rocks with rich internal voids. Next, we will focus on the description effect of this model on the creep behavior of other rocks and further modify it to adapt to more rocks

Data Availability

The data used to support the findings of this research are included within the paper.

Conflicts of Interest

The authors declare no conflict of interest.

Authors' Contributions

The contributions to the work performed in this article were as follows: Qingheng Gu designed the project with the help of Guangming Zhao and Xiangrui Meng. Qingheng Gu, Jian Sun, Xiang Cheng, and Wensong Xu contributed to the preparation of the manuscript. Creep experiments and scanning electron microscope test were performed by Qingheng Gu and Ruofei Zhang. Zhao Guangming and Xiangrui Meng provided establishment method of creep model.

Acknowledgments

This research was funded by the Anhui Provincial Natural Science Foundation (No. 2208085QE143), National Natural Science Foundation of China (Nos. 51974009 and 52004005), Anhui Province Science and Technology Major Project (No. 202203a07020011), Anhui Province "Provincial Special Expenditure Plan" Leading Talent Project (No. T000508), Collaborative Innovation Project of Anhui Province Universities (GXXT-2021-075), Scientific Research Activities of Academic and Technical Leaders in Anhui Province, Huaibei City Science and Technology Major Program (Z2020005), Postdoctoral Science Foundation of Anhui Province (No. 2021B513), Scientific Research Start-up Fund for High-Level Talent Introduction of AUST (No. 13210658), Anhui Engineering Research Center of Exploitation and Utilization of Closed/Abandoned Mine Resources (No. EUCMR202203) and Independent Research fund of the State Key Laboratory of Mining Response and Disaster Prevention and Control in Deep Coal Mines, Anhui University of Science and Technology (No. SKLMRDPC19ZZ012).

References

[1] J. G. Ning, J. Wang, Y. L. Tan, L. S. Zhang, and T. T. Bu, "In situ investigations into mining-induced overburden failures in close multiple-seam longwall mining: a case study," *Geomechanics and Engineering*, vol. 12, no. 4, pp. 657–673, 2017.

[2] Z. G. Tao, C. Zhu, X. H. Zheng et al., "Failure mechanisms of soft rock roadways in steeply inclined layered rock formations," *Geomatics Natural Hazards and Risk*, vol. 9, no. 1, pp. 1186–1206, 2018.

[3] Q. Liu, Y. J. Sun, and J. Li, "Experimental study on seepage characteristics of Jurassic weakly cemented sandstone under water-rock interaction," *Geofluids*, vol. 2020, Article ID 8543687, 12 pages, 2020.

[4] J. H. Zhang, L. G. Wang, Q. H. Li, and S. S. Zhu, "Plastic zone analysis and support optimization of shallow roadway with weakly cemented soft strata," *International Journal of Mining Science and Technology*, vol. 25, no. 3, pp. 395–400, 2015.

[5] Y. L. Tan, X. S. Liu, J. G. Ning, and Y. W. Lu, "In situ investigations on failure evolution of overlying strata induced by mining multiple coal seams," *Geotechnical Testing Journal*, vol. 40, no. 2, pp. 20160090–20160257, 2017.

[6] Q. L. Yao, T. Chen, M. H. Ju, S. Liang, Y. P. Liu, and X. H. Li, "Effects of water intrusion on mechanical properties of and crack propagation in coal," *Rock Mechanics and Rock Engineering*, vol. 49, no. 12, pp. 4699–4709, 2016.

[7] G. Fabre and F. Pellet, "Creep and time-dependent damage in argillaceous rocks," *International Journal of Rock Mechanics and Mining Sciences*, vol. 43, no. 6, pp. 950–960, 2006.

[8] P. Cao, L. H. Wan, Y. X. Wang, Y. H. Huang, and X. Y. Zhang, "Viscoelasto-plastic properties of deep hard rocks under water environment," *Transactions of Nonferrous Metals Society of China*, vol. 21, no. 12, pp. 2711–2718, 2011.

[9] B. Q. Yan, Q. F. Guo, F. H. Ren, and M. F. Cai, "Modified Nishihara model and experimental verification of deep rock mass under the water-rock interaction," *International Journal of Rock Mechanics and Mining Sciences*, vol. 128, article 104250, 2020.

[10] Y. C. Wang, Y. Liu, Y. L. Li, W. Jiang, and Y. M. Wang, "Experimental study on the failure mechanism of tunnel surrounding rock under different groundwater seepage paths," *Geofluids*, vol. 2021, Article ID 8856365, 17 pages, 2021.

[11] Q. L. Yao, C. J. Tang, Z. Xia et al., "Mechanisms of failure in coal samples from underground water reservoir," *Engineering Geology*, vol. 267, article 105494, 2020.

[12] C. Yu, S. Tang, C. Tang et al., "The effect of water on the creep behavior of red sandstone," *Engineering Geology*, vol. 253, pp. 64–74, 2019.

[13] Z. Luo, J. Li, Q. Jiang et al., "Effect of the water-rock interaction on the creep mechanical properties of the sandstone rock," *Periodica Polytechnica-Civil Engineering*, vol. 62, no. 2, pp. 451–461, 2015.

[14] C. J. Tang, Q. L. Yao, Z. Y. Li, Y. Zhang, and M. H. Ju, "Experimental study of shear failure and crack propagation in water-bearing coal samples," *Energy Science and Engineering*, vol. 7, pp. 2193–2204, 2018.

[15] S. T. Ji, Z. Wang, and J. Karlovšek, "Analytical study of subcritical crack growth under mode I loading to estimate the roof durability in underground excavation," *International Journal of Mining Science and Technology*, vol. 32, no. 2, pp. 375–385, 2022.

[16] J. F. Ju, Q. S. Li, and J. L. Xu, "Experimental study on the self-healing behavior of fractured rocks induced by water-CO_2-rock interactions in the Shendong coalfield," *Geofluids*, vol. 2020, Article ID 8863898, 14 pages, 2020.

[17] H. F. Ma, Y. Q. Song, S. J. Chen et al., "Experimental investigation on the mechanical behavior and damage evolution mechanism of water-immersed gypsum rock," *Rock Mechanics and Rock Engineering*, vol. 54, no. 9, pp. 4929–4948, 2021.

[18] D. X. Li, E. Y. Wang, X. G. Kong, X. R. Wang, C. Zhang, and H. S. Jia, "Fractal characteristics of acoustic emissions from coal under multi-stage true-triaxial compression," *Journal of Geophysics and Engineering*, vol. 15, pp. 2021–2032, 2018.

[19] W. R. Liu, W. Yuan, Y. T. Yan, and X. Wang, "Analysis of acoustic emission characteristics and damage constitutive model of coal-rock combined body based on particle flow code," *Symmetry*, vol. 11, no. 8, p. 1040, 2019.

[20] R. D. Lei, F. Berto, C. Hu, Z. H. Lu, and X. F. Yan, "Early-warning signal recognition methods in flawed sandstone subjected to uniaxial compression," *Fatigue and Fracture of Engineering Materials and Structures*, vol. 13911, pp. 1–20, 2022.

[21] X. Wang, W. Yuan, Y. T. Yan, and X. Zhang, "Scale effect of mechanical properties of jointed rock mass: a numerical study based on particle flow code," *Geomechanics and Engineering*, vol. 21, no. 3, pp. 259–268, 2020.

[22] G. Q. Chen, H. Li, T. Wei, and J. Zhu, "Searching for multi-stage sliding surfaces based on the discontinuous dynamic strength reduction method," *Engineering Geology*, vol. 286, article 106086, 2021.

[23] G. Q. Chen, P. Tang, R. Q. Huang, and D. Wang, "Critical tension crack depth in rockslides that conform to the three-section mechanism," *Landslides*, vol. 18, no. 1, pp. 79–88, 2021.

[24] X. Z. Wu, Y. J. Jiang, and Z. C. Guan, "A modified strain-softening model with multi-post-peak behaviours and its application in circular tunnel," *Engineering Geology*, vol. 240, pp. 21–33, 2018.

[25] S. T. Ji and J. Karlovšek, "Calibration and uniqueness analysis of microparameters for DEM cohesive granular material," *International Journal of Mining Science and Technology*, vol. 32, no. 1, pp. 121–136, 2022.

[26] F. Tahmasebinia, C. G. Zhang, I. Canbulat, O. Vardar, and S. Saydam, "Computing the damage and fracture energy in a coal mass based on joint density," *International Journal of Mining Science and Technology*, vol. 28, no. 5, pp. 813–817, 2018.

[27] G. C. Shi, X. J. Yang, H. C. Yu, and C. Zhu, "Acoustic emission characteristics of creep fracture evolution in double-fracture fine sandstone under uniaxial compression," *Engineering Fracture Mechanics*, vol. 210, pp. 13–28, 2019.

[28] Y. K. Ma, Q. C. Yao, J. H. Wang, S. Sun, and Z. L. Qiu, "Time-dependent creep constitutive model of roadway surrounding rock based on creep parameters," *Geofluids*, vol. 2022, Article ID 7981192, 11 pages, 2022.

[29] J. Z. Tang, S. Q. Yang, D. Elsworth, and Y. Tao, "Three-dimensional numerical modeling of grain-scale mechanical behavior of sandstone containing an inclined rough joint," *Rock Mechanics and Rock Engineering*, vol. 54, no. 2, pp. 905–919, 2021.

[30] ISRM, "Rock characterization, testing and monitoring," in *ISRM (International Society for Rock Mechanics) Suggested Methods*, E. T. Brown, Ed., Pergamon, Oxford, 1981.

[31] Q. H. Gu, Q. Ma, Y. L. Tan, Z. C. Jia, Z. H. Zhao, and D. M. Huang, "Acoustic emission characteristics and damage model of cement mortar under uniaxial compression," *Construction and Building Materials*, vol. 213, pp. 377–385, 2019.

[32] W. Y. Guo, F. H. Yu, Y. L. Tan, and T. B. Zhao, "Experimental study on the failure mechanism of layer-crack structure," *Energy Science and Engineering*, vol. 7, no. 6, pp. 2351–2372, 2019.

[33] X. Wang and L. G. Tian, "Mechanical and crack evolution characteristics of coal-rock under different fracture-hole conditions: a numerical study based on particle flow code," *Environmental Earth Sciences*, vol. 77, no. 8, p. 297, 2018.

[34] F. Q. Ren, C. Zhu, and M. C. He, "Moment tensor analysis of acoustic emissions for cracking mechanisms during schist strain burst," *Rock Mechanics and Rock Engineering*, vol. 53, no. 1, pp. 153–170, 2020.

[35] X. P. Zhang, Y. J. Jiang, G. Wang et al., "Mechanism of shear deformation, failure and energy dissipation of artificial rock joint in terms of physical and numerical consideration," *Geosciences Journal*, vol. 23, pp. 519–529, 2020.

[36] J. Z. Tang, S. Q. Yang, Y. L. Zhao, and W. L. Tian, "Experimental and numerical modeling of the shear behavior of filled rough joints," *Computers and Geotechnics*, vol. 17, pp. 2084–2097, 2022.

[37] Y. L. Tan, Q. H. Gu, J. G. Ning, X. S. Liu, Z. C. Jia, and D. M. Huang, "Uniaxial compression behavior of cement mortar and its damage-constitutive model based on energy theory," *Materials*, vol. 12, no. 8, p. 1309, 2019.

[38] N. N. Danesh, Z. W. Chen, L. D. Connell, M. S. Kizil, Z. J. Pan, and S. M. Aminossadati, "Characterisation of creep in coal and its impact on permeability: an experimental study," *International Journal of Coal Geology*, vol. 173, pp. 200–211, 2017.

[39] H. P. Xie, *Damage Mechanics of Rock and Concrete*, China University of Mining and Technology Press, Xuzhou, 1990.

[40] J. B. Zhu, B. Wang, and A. Q. Wu, "Study of unloading triaxial rheological tests and its nonlinear damage constitutive model of Jinping hydropower station green sandstone," *Chinese Journal of Rock Mechanics and Engineering*, vol. 29, pp. 528–534, 2010, (in Chinese).